



www.shd.org.rs

*J. Serb. Chem. Soc.* 73 (8–9) 861–870 (2008)

JSCS–3768

JSCS@tmf.bg.ac.yu • www.shd.org.rs/JSCS

UDC 669.1–492.2+66.087:541.135–32

Original scientific paper

## Electrodeposition of Fe powder from acid electrolytes

VESNA M. MAKSIMOVIĆ<sup>1\*</sup>, LJUBICA J. PAVLOVIĆ<sup>2#</sup>,  
BORKA M. JOVIĆ<sup>3#</sup> and MIOMIR G. PAVLOVIĆ<sup>2#</sup>

<sup>1</sup>*Institute of Nuclear Sciences Vinča, University of Belgrade, P.O. Box 522, 11000 Belgrade,*

<sup>2</sup>*Institute of Electrochemistry ICTM, University of Belgrade, Njegoševa 12, 11000 Belgrade,*

*and* <sup>3</sup>*Institute for Multidisciplinary Research, P.O. Box 33, 11030 Belgrade, Serbia*

(Received 17 December 2007, revised 27 February 2008)

**Abstract:** Polarization characteristics of the electrodeposition processes of Fe powders from sulfate and chloride electrolytes and the morphology of the obtained powders were investigated. The morphology depended on the anion presence in the electrolyte but not on the current density in the investigated range. A characteristic feature of the dendritic powder with cauliflower endings obtained from sulfate electrolyte is the presence of cone-like cavities and the crystallite morphology of the powders surface. On the other hand, Fe powders electrodeposited from chloride electrolyte appear in the form of agglomerates. A soap solution treatment applied as a method of washing and drying provides good protection from oxidation of the powders.

**Keywords:** Fe powder; morphology; polarization diagrams.

### INTRODUCTION

By the electrochemical classification of metals, transition metals such as Fe, Ni and Co belong to the "inert metal" group, with a small exchange current density,  $j_0$ , and a high overpotential of electrodeposition,  $\eta$ .<sup>1,2</sup> All polarization diagrams recorded during the electrochemical deposition of metals and alloy powders of the Fe group are distinguished through the following phenomena: a) the deposition of powders (as well as compact metal) is accompanied by the simultaneous evolution of hydrogen from the very beginning of metal deposition. In this situation, a plateau corresponding to the limiting current density cannot be registered on the polarization diagram, as is the case with copper,<sup>3</sup> b) all of the polarization diagrams corrected for the  $IR$  drop are characterized by the presence of two inflexion points, *i.e.*, the first inflection corresponds to the beginning of metal deposition, which is then followed by a rapid rise of the current density, where-

\* Corresponding author. E-mail: vesnam@vin.bg.ac.yu

# Serbian Chemical Society member.

doi: 10.2298/JSC0809861M

as the second inflection characterizes the start of a linear change of current density with potential. This deviation from linearity demonstrates a change of the mechanism of metal deposition.<sup>4,5</sup>

Fe powder is an important raw material, which is widely used in the manufacture of porous metallo–ceramic bearings, friction materials, parts for machinery, for production of various alloys, in the chemical industry for the fabrication of rechargeable batteries, *etc.*<sup>6</sup> The physical and chemical characteristics of Fe determine its peculiar electrochemical behavior. Almost all data concerning the electrodeposition of Fe powders were summarized by Calusaru.<sup>6</sup> A literature survey of the electrodeposition of Fe powders shows that mainly two types of electrolytes were investigated and these were based on sulfate<sup>6–11</sup> and chloride electrolytes.<sup>6,12</sup> In all the reported cases, the morphology of the deposited powders was dendritic.<sup>8,13</sup> With increasing duration of electrolysis, the dendrites merge, which is unacceptable for the further application of such deposits as they must be ground in order to obtain powders. However, in the range of lower acidity, the deposits become powdery and, in some cases, may be spongy and sticky. Generally, the hitherto research indicates that there are two steps in the electrodeposition of Fe powders, deposition of a fragile film followed by grinding.<sup>14–16</sup> It should be emphasized that we successfully attempted to obtain powdery Fe powders without the grinding process.

Fe powders have a very high tendency to corrosion. The wet electrolytic product contains over 99 % Fe, while the washed and dried powders may contain several percent of oxide.<sup>8</sup> Kuzmin and Kiseleva<sup>8</sup> demonstrated a marked influence of pH on the content of oxide in Fe powders electrodeposited from sulfate electrolytes. Fe(II)-based electrolytes were investigated within the pH range 1.5–4.2. The oxide content depended not only on the amount of hydroxides formed during deposition, but also on the amount of powder oxidized during washing and drying. It is noteworthy that the lower the pH, the much lower was the oxide content.

The aim of this work was to investigate the polarization characteristics of the processes of the electrodeposition of Fe powders from sulfate and chloride electrolytes and the morphologies of the obtained powder as a function of the type of electrolyte and current density. X-Ray diffraction analysis was performed in order to check the quality of the selected way of stabilization of the Fe powders.

#### EXPERIMENTAL

Polarization diagrams were recorded in a three-compartment standard electrochemical cell at room temperature. The Pt-foil counter electrode and the reference saturated silver|silver chloride (Ag|AgCl) electrode were placed in separated compartments. All solutions were prepared from analytical grade chemicals and distilled water. Polarization measurements were performed using a computer-controlled potentiostat (PAR M273A) and corrosion software (PAR M352/252, Version 2.01) at a sweep rate of 1.0 mV s<sup>-1</sup>. To obtain polarization curves corrected for the *IR* drop, the current interrupt technique was used with a current interruption time of 0.5 s.

All powder samples were electrodeposited at the room temperature in a cylindrical glass cell of total volume 3 dm<sup>3</sup> with a cone-shaped bottom for the collection of the powder particles. The working electrode was a glassy carbon rod with a total surface area of 1.45 cm<sup>2</sup> immersed in the solution and placed in the middle of the cell.

Pure metal powders were electrodeposited from solutions containing either 70 g dm<sup>-3</sup> FeSO<sub>4</sub> + 133 g dm<sup>-3</sup> (NH<sub>4</sub>)<sub>2</sub>SO<sub>4</sub> or 50 g dm<sup>-3</sup> FeCl<sub>2</sub> + 105 g dm<sup>-3</sup> NH<sub>4</sub>Cl. The deposition time was 5.0 min. The pH of the investigated solutions was varied from 1.3 to 1.6.

The wet powder was washed several times with a large amount of demineralized water until the wet powder was free from traces of acid. All the time, the powder was submerged in water to prevent oxidation. To inhibit oxidation in air, sodium soap Sap G-30, which contains 78 % of total fatty acids, was added as an additive to the water used for washing the Fe powder. The powder was then dried in the a furnace under a controlled nitrogen atmosphere at 100 °C.<sup>17</sup>

The morphology of the electrodeposited powders was examined using a Jeol T-20 scanning electron microscope, SEM.

The phase structure of the powders was investigated using a Philips PW 1050 X-ray powder diffractometer.

#### RESULTS AND DISCUSSION

It is well-known that the deposition of powders (as well as compact metal) of the Fe group is accompanied by the simultaneous evolution of hydrogen from the very beginning of metal deposition. A selection of the polarization diagrams for the process of electrodeposition of Fe powders from chloride electrolyte, the polarization curve for the electrodeposition of Fe powder measured with correction for the *IR* drop (Fe + H<sub>2</sub>), the polarization curve for hydrogen evolution (H<sub>2</sub>) and the polarization curve for Fe powder electrodeposition after subtraction of *j*<sub>H<sub>2</sub></sub> (Fe) are shown in Fig. 1a. The current for hydrogen evolution was obtained using the equation for the Faraday law<sup>18</sup> applied to the process of gas evolution:

$$I_{\text{H}_2} = \frac{nFV_0}{tV_n} \quad (1)$$

where *V*<sub>0</sub> is the experimentally determined volume of evolved hydrogen at *p*<sub>at</sub> and *T* = 298 K corrected to normal conditions (*p*<sup>⊖</sup> and *T* = 273 K), *t* the time of hydrogen evolution at a constant current, *V*<sub>n</sub> the volume of 1 mol of hydrogen at normal conditions (22.4 dm<sup>3</sup> mol<sup>-1</sup>), *n* the number of exchanged electrons and *F* is the Faraday constant. After subtracting the obtained values from the total current densities (Fe + H<sub>2</sub>), the values corresponding to the deposition of pure iron (Fe) were obtained. All polarization diagrams are characterized by the presence of two inflection points.

The current efficiency for the electrodeposition process was obtained from the relation:

$$\eta_j(\%) = 100 \frac{j_{\text{Fe}/\text{SO}_4^{2-}}}{j_{\text{tot}}} = 100 \frac{j_{\text{tot}} - j_{\text{H}_2}}{j_{\text{tot}}} \quad (2)$$

The corresponding values of the current efficiency are shown in Fig. 1b. As can be seen at the beginning of the electrodeposition process significant amount of hydrogen is evolving, causing the value of the current efficiency of about 30 %. At more negative potentials this value increases to about 55 % and further the sharp decrease is taking place in the region of the sharp increase in current density to about more than 30 %.

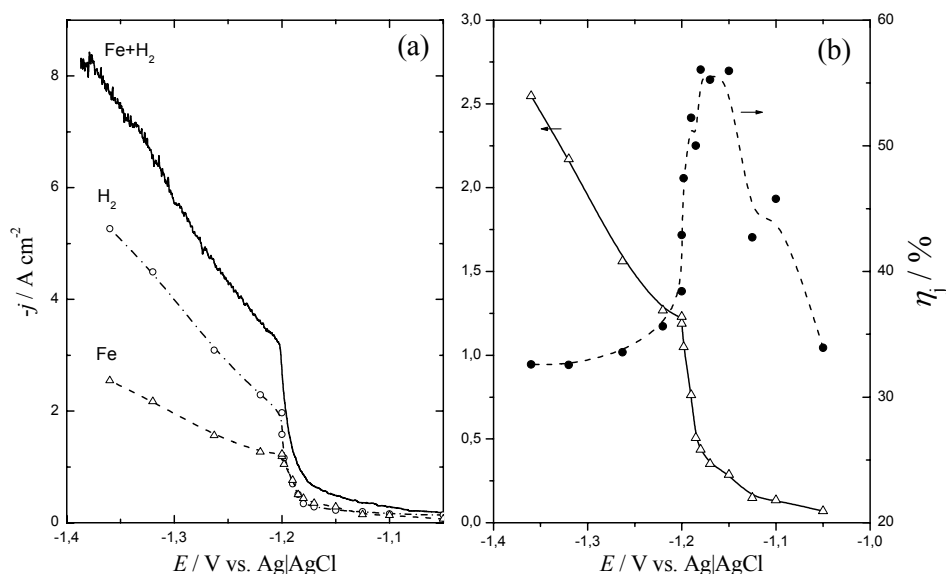


Fig. 1. (a) Polarization curve for the electrodeposition of Fe powder from the chloride electrolyte measured with  $IR$  drop correction (solid line  $Fe + H_2$ ), ( $\circ$ ) polarization curve for hydrogen evolution (dashed-dotted line,  $H_2$ ) and ( $\Delta$ ) polarization curve for Fe powder electrodeposition after subtraction of  $j_{H_2}$  (dashed line,  $Fe$ ); (b) polarization curve for Fe powder electrodeposition and the corresponding  $\eta_j$  vs.  $E$  curve ( $\bullet$ ).

The polarization diagrams ( $Fe + H_2$ ) for the processes of electrodeposition of Fe powders from sulfate and chloride electrolytes are illustrated in Fig. 2. A sharp increase of the current occurred at about  $-1.0$  V during the deposition from sulfate electrolyte, while for the deposition from chloride electrolyte, this phenomenon moved to more negative potentials (at about  $-1.2$  V), indicating that the overpotential for the deposition from chloride electrolyte is by about  $0.20$  V negative than that from the sulfate electrolyte. The shape of the diagrams suggests that intensive hydrogen evolution occurred during the deposition process. According to the polarization diagrams, three current densities for each electrolyte were selected for analysis (see Fig. 2).

The morphology of the obtained powders depended on the anion presence in the electrolyte. The typical morphology of the powder electrodeposited from sulfate and chloride electrolytes is shown in Figs. 3a and 3b, respectively. The Fe

powder electrodeposited from the sulfate electrolyte was characterized by dendrite, coral-like particles, while the powder electrodeposited from the chloride electrolyte contained one type of agglomerates.

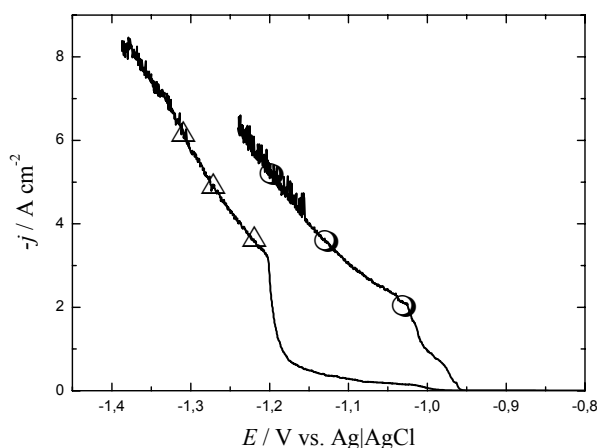


Fig. 2. Polarization curves for the electrodeposition of Fe powders from the sulfate and chloride electrolytes measured with  $IR$  drop correction at selected current densities; ( $\Delta$ ) chloride ( $j = 3.6, 4.8$  and  $6.0 \text{ A cm}^{-2}$ ) and ( $\circ$ ) sulfate ( $j = 2, 3.5$  and  $5.0 \text{ A cm}^{-2}$ ) electrolytes.

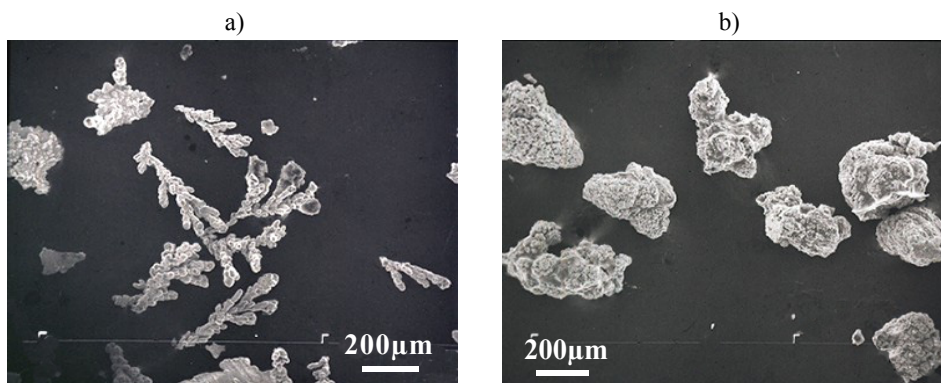


Fig. 3. Typical powder particle morphology; sulfate,  $j = 5.0 \text{ cm}^{-2}$  (a), and (b) chloride electrolyte,  $j = 6.0 \text{ A cm}^{-2}$ .

The morphologies of the Fe powders and their surfaces deposited from the sulfate electrolyte at current densities  $j = 2, 3.5$  and  $5.0 \text{ A cm}^{-2}$  are shown in Figs. 4a–4f. The morphology of the Fe powders deposited at all the investigated current densities is dendritic of the coral type. There is no significant difference in size and shape of particles with increasing current density in the range from  $2.0$  to  $5.0 \text{ A cm}^{-2}$ . Only primary ramification of the dendrites occurred without a clear crystallographic orientation and further ramification was hindered. It is a characteristic for the primary branch of dendritic particles that only one type of cavity, *i.e.*, cone-shaped, could be detected on all the particles: (Fig. 4b). The appearance of such cavities is most probably the result of bubble formation due to

hydrogen evolution.<sup>4,5,19</sup> Such a kind of cavities was found and explained in previous papers on alloy powders.<sup>4,5</sup> At higher magnification, which enabled detailed observation of the morphology of the dendrite, insufficiently developed cauliflower endings with crystallites were noticed regardless of the applied current density. These crystallites represent potential places for further growth of dendrites. The morphology of the endings depends on the moment of detachment of the particles from the electrode.<sup>4</sup>

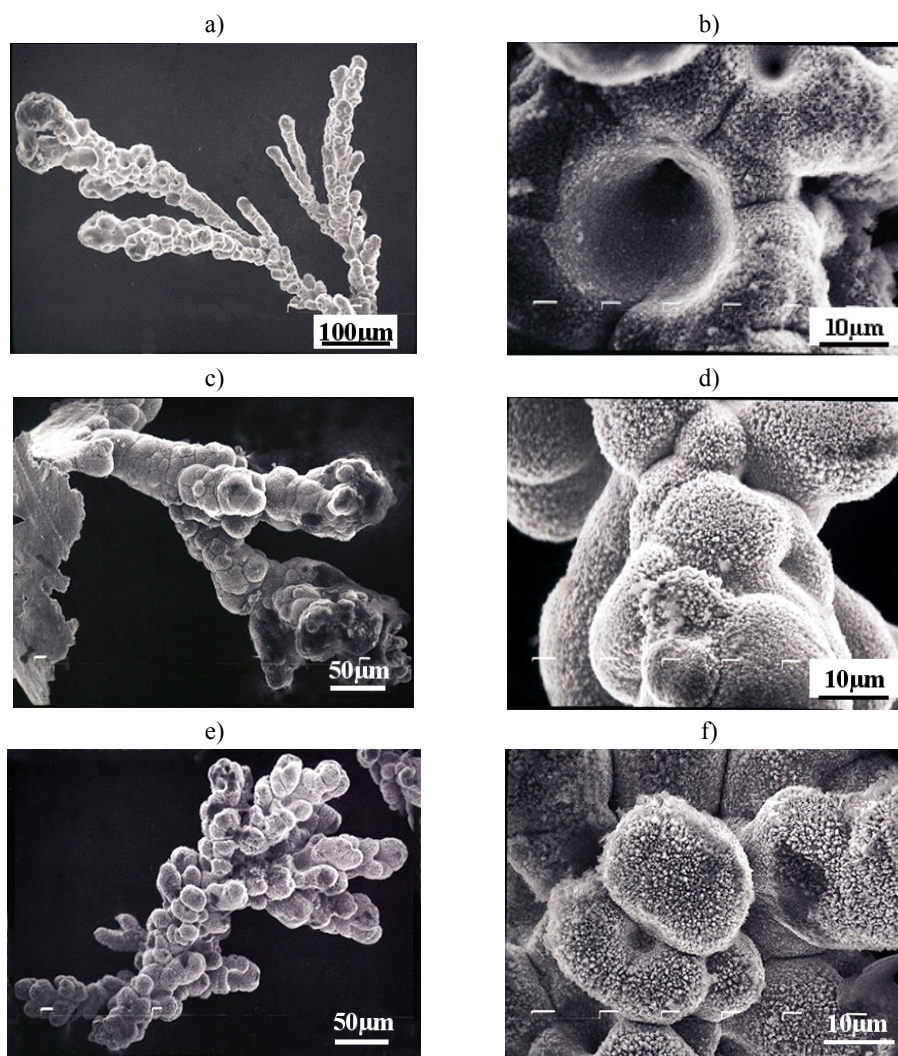


Fig. 4. SEM Micrographs of Fe powders electrodeposited from sulfate electrolyte: morphology of the powder particles (a, c, e); morphology of the surface (b, d, f);  $j = 2.0$  (a, b),  $3.5$  (c, d) and  $5.0 \text{ A cm}^{-2}$  (e, f).

The morphologies of the Fe powder particles and of their surfaces deposited from chloride electrolyte at current densities  $j = 3.6, 4.8$  and  $6.0 \text{ A cm}^{-2}$  are shown in Figs. 5a–5f. In this case, only agglomerates were detected at all the investigated current densities. Some of these agglomerates were spherical (Fig. 5a). The higher magnification microphotographs (Figs. 5b, 5d and 5f) reveal that the top surface of these agglomerates also had cauliflower-like endings. The main characteristic of the top surface of these particles was the presence of crystallites on the cauliflower-like endings. Such a morphology indicates that a second layer of growth of nodules occurred.<sup>19</sup>

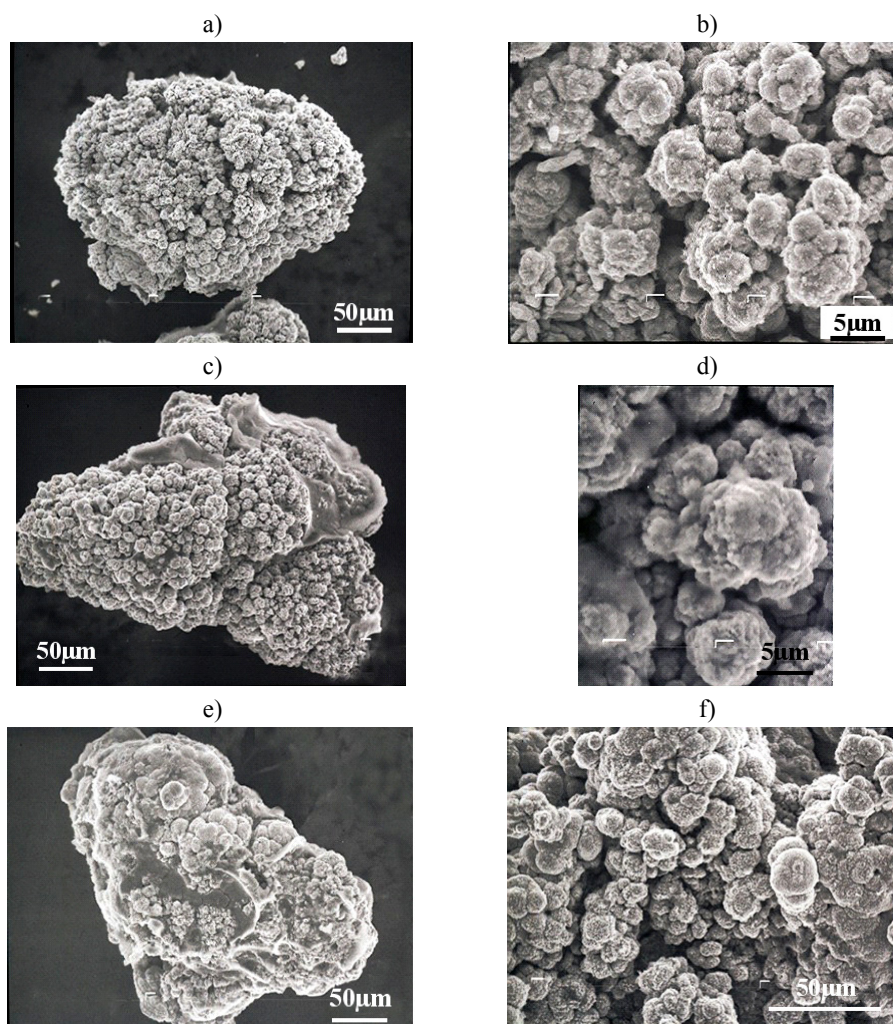


Fig. 5. SEM Micrographs of Fe powders electrodeposited from chloride electrolyte: morphology of powder (a, c, e); morphology of surface (b, d, f);  $j = 3.6$  (a, b),  $4.8$  (c, d) and  $6.0 \text{ A cm}^{-2}$  (e, f).

Powders have a high chemical activity because of their large surface area and, hence, readily react with the oxygen in air to form surface oxides.<sup>6,14,20</sup> It is known that corrosion processes occur at the boundary of the surface of the powder particles and the liquid phase. In this way, it is possible to imagine that moisture adsorption can be prevented by the formation of a film on the surface of the powder particles, which could enable their long-term and safe protection. In relation to this, it was necessary to find stabilizers that would enable the creation of hydrophobic adsorption films on the surface of the powder particles, which would be able to protect and stabilize the metal surface from the effect of moisture.<sup>17,20</sup> It was found that benzoic acid, Sap G-30 and benzotriazol were the best stabilizers for copper particles.<sup>17</sup> The assumption is that they stabilize by forming colloidal precipitates in the form of a protective film on the surface of the particles. The X-ray diffractograms of Fe powders deposited from sulfate and chloride electrolytes and stabilized by sodium soap are shown in Fig. 6. Throughout the investigated range of  $2\theta$ , the X-ray patterns contain only two characteristic peaks, corresponding to the  $\alpha$ -Fe phase with a body-centered cubic (bcc) crystal lattice with (110) and (200) planes. It should be pointed out that reflections of possibly present oxides ( $\text{FeO}$ ,  $\text{Fe}_2\text{O}_3$  and  $\text{Fe}_3\text{O}_4$ ) were not detected in either of the two samples, which proves that the soap solution treatment applied as a method of washing and drying provided good protection of the Fe powders from oxidation.

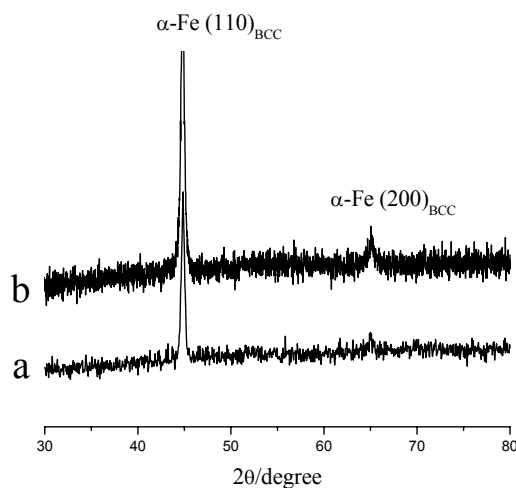


Fig. 6. X-Ray diffractograms of Fe powders electrodeposited from: a) sulfate electrolyte at  $j = 5.0 \text{ A cm}^{-2}$ , and b) chloride electrolyte at  $j = 6.0 \text{ A cm}^{-2}$ .

#### CONCLUSIONS

The main results obtained in this study can be summarized as follows:

1. Polarization diagrams recorded during the electrochemical deposition of Fe powders were characterized by the presence of two inflexion points, *i.e.*, the



first inflection corresponded to the beginning of metal deposition which is then followed by a rapid rise in the current density, whereas the second inflection characterizes the start of the linear change of the current density with potential.

2. The morphology and composition of the obtained powders depended on the anion presence in the electrolyte. Generally, two types of particles could be distinguished: dendrites (sulfate electrolyte) and agglomerates (chloride electrolyte) at all the investigated current densities.

3. The main characteristic of the top surface of all particles was the presence of crystallites on the cauliflower endings.

4. Cavities, which were the result of bubble formation due to hydrogen evolution, could be found only in the powders electrodeposited from the sulfate electrolytes.

5. The X-ray patterns contained only characteristic peaks corresponding to the  $\alpha$ -Fe phase, indicating that the quality of the selected method of stabilization using a soap solution gave good protection from oxidation.

*Acknowledgment.* This work was financially supported by the Ministry of Science of the Republic of Serbia under the research project "Deposition of ultrafine powders of metals and alloys and nanostructured surfaces by electrochemical techniques" (142032G/2006).

#### ИЗВОД

#### ЕЛЕКТРОХЕМИЈСКО ТАЛОЖЕЊЕ Fe ПРАХОВА ИЗ КИСЕЛИХ ЕЛЕКТРОЛИТА

ВЕСНА М. МАКСИМОВИЋ<sup>1</sup>, ЉУБИЦА Ј. ПАВЛОВИЋ<sup>2</sup>, БОРКА М. ЈОВИЋ<sup>3</sup> и МИОМИР Г. ПАВЛОВИЋ<sup>2</sup>

<sup>1</sup>Институт за нуклеарне науке "Винча", б. бр. 522, 11000 Београд, <sup>2</sup>ИХТМ, Центар за електрохемију, Универзитет у Београду, Њеђошева 12, 11000 Београд и <sup>3</sup>Институт за мултидисциплинарна истраживања, б. бр. 33, 11030 Београд

У овом раду приказани су резултати испитивања поларizacionих карактеристика процеса таложења Fe прахова из сулфатних и хлоридних електролита, као и морфологија добијеног праха. Утврђено је да морфологија честица зависи од врсте анјона присутних у електролиту, али не и од примењене густине струје у испитиваном опсегу. Карактеристично за честице које су исталожене из сулфатних електролита је да су оне дендритичне са карфиоластим, кристалиничним завршцима и да поседују купасте шупљине. Код Fe прахова исталожених из хлоридних електролита уочени су агломерати. Коришћење раствора сапуна у процесу прања и сушења прахова показао се као добар метод заштите праха од оксидације.

(Примљено 17. децембра 2007, ревидирано 27 фебруара 2008)

#### REFERENCES

1. R. Piontelli, in *Proceedings of 2<sup>nd</sup> Meeting of CITCE*, (1950), Milan, Italy, (1951), p. 163
2. S. Tajima, M. Ogata, *Electrochim. Acta* **13** (1968) 1845
3. N. D. Nikolić, Lj. J. Pavlović, M. G. Pavlović, K. I. Popov, *J. Serb. Chem. Soc.* **72** (2007) 1369
4. V. D. Jović, B. M. Jović, V. Maksimović, M. G. Pavlović, *Electrochim. Acta* **52** (2007) 4254
5. V. D. Jović, B. M. Jović, M. G. Pavlović, *Electrochim. Acta* **51** (2006) 5468

6. A. Calusaru, *Electrodeposition of Powders from Solutions*, Elsevier, New York, NY, 1979, p. 363
7. N. Kudryavtsev, V. Petrovna, *Novosti tehniki*, N. K. T. R. **171** (1932) (in Russian)
8. L. Kuzmin, V. Kiseleva, *Zhur. Prikl. Khim.* **22** (1949) 311 (in Russian)
9. C. Hardy, C. Mantell, F. Patent, 814500 (1937)
10. C. Hardy, C. Mantell, US Patent, 2157699 (1938)
11. N. Kurdyavtsev, E. Tereshkovitch, *Zhur. Prikl. Khim.* **21** (1948) 1298 (in Russian)
12. M. Balshin, *NIIMASH* **12** (1935) 5
13. H. Casey, US Patent, 2481079 (1949)
14. I. A. Carlos, C. S. Caruso, *J. Power Sources* **73** (1998) 199
15. M. L. Trudeau, *Nanostruct. Mater.* **12** (1999) 55
16. P. K. Samal, E. Klar, US Patent, 4134800 (1979)
17. M. G. Pavlović, Lj. J. Pavlović, I. D. Doroslovački, N. D. Nikolić, *Hydrometallurgy* **74** (2004) 155
18. F. A. Lowenheim, *Modern Electroplating*, 3<sup>rd</sup> Ed., Wiley, New York, 1974
19. V. D. Jović, V. Maksimović, M. G. Pavlović, K. I. Popov, *J. Solid State Electrochem.* **10** (2006) 373
20. A. I. Levin, A. V. Pomosov, *Zhur. Prikl. Khim.* **23** (1950) 949 (in Russian).